How to cite: *Angew. Chem. Int. Ed.* **2024**, *63*, e202404014
doi.org/10.1002/anie.202404014

One-Dimensional Wires

Aggregation of One-Dimensional Wires: The Case of Long Oligoynes

Fernando Gordillo-Gámez[+], Yueze Gao[+], Juan Aragó, Enrique Ortí, Daniel Aranda, Miklos Kertesz,* Rik R. Tykwinski,* and Juan Casado**

Abstract: We show an unexpected aggregation phenomenon of a long oligoyne (**Py[16]**) with 16 contiguous triple bonds and endcapped with bulky 3,5-bi(3,5-bis-*tert*-butylphenyl)pyridine groups. Aggregation of 1D π-conjugated oligoyne chains is rare given the minimal π–π intermolecular interactions as well as its flexibility that works against self-assembly. In dilute solutions, the reversible aggregation of **Py[16]** initiates at low temperature in the range of 140–180 K, and is not observed for shorter oligoynes in this series. Cryogenic UV/Vis electronic absorption spectra and vibrational Raman spectra with different laser wavelength lines tuning from in-resonance to off-resonance conditions have been used to extract the vibrational features characterizing the monomer and aggregate species. Theoretical calculations complement the spectroscopic findings.

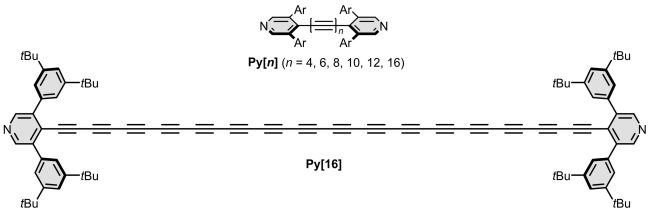

Scheme 1. Chemical formula of the **Py[*n*]** oligoynes together with the extended chemical structure of **Py[16]**.

Oligoynes[1] are 1-dimensional (1D) wires made of *sp*-hybridized carbon atoms and are viewed as molecular models of a new allotrope of naturally existing carbon, carbyne, i.e., the infinite oligoyne chain.[2] In the effort to assemble the longest possible oligoynes in order to mimic the structural and electronic properties of carbyne, a series of oligoynes of increasing length with bulky 3,5-bi(3,5-bis-*tert*-butylphenyl)pyridine as endgroups has been synthesized (**Py[*n*]**, Scheme 1).[3] Until very recently,[4] **Py[*n*]** were the longest reported polyynes and offered an opportunity to explore physical behavior that had not previously been possible. Here we report unexpected findings for the aggregation behavior of **Py[16]**, namely, the oligoyne of this series with 16 contiguous triple bonds.

Among the large variety of aggregation phenomena displayed by organic molecules, 2D-polycyclic aromatic nanographenes have received special attention since the structural rigidity imparted by planarity and the large available planar π-surface facilitate π–π interactions that provide the driving force for aggregation.[5,6,7]

On the one hand, aggregation is one of the main problems in the chemical characterization of large polyaromatics since it hinders the use of standard techniques of chemical analysis (e.g., NMR spectroscopy requires homogeneous solutions).[8] On the other hand, knowledge and control of aggregation plays a fundamental role in the design of solid-state structures for which supramolecular and crystalline order are required. In the case of planar molecules, π–π interactions are magnified by the available flat surfaces (perylene is a prototypical case, Figure 1[7]). Aggregation of 3D molecules, such as C_{60} fullerene, has been widely studied and correlated with its physical and electronic properties.[9] In contrast to aggregation of 2D and 3D molecules, π–π induced aggregation is hard to envisage in 1D molecular systems such as oligoynes. The greater flexibility[10] and the minimal π-surface of 1D systems limit the intermolecular enthalpic forces needed to surpass the entropic price of self-assembly. As would thus be expected, aggregation effects in 1D molecules are rare, and studies to explore aggregation in 1D systems are challenging, often requiring cryogenic experiments in order overcome entropic disorder.

[*] F. Gordillo-Gámez,[+] Prof. J. Casado
Department of Physical Chemistry, University of Málaga, Andalucia-Tech Campus de Teatinos s/n, 29071 Málaga, Spain
E-mail: casado@uma.es

Dr. Y. Gao,[+] Prof. R. R. Tykwinski
Department of Chemistry, University of Alberta, Edmonton, Alberta, T6G 2G2 Canada
E-mail: rik.tykwinski@ualberta.ca

Dr. J. Aragó, Prof. E. Ortí, Dr. D. Aranda
Instituto de Ciencia Molecular (ICMol), Universitat de València, 46980 Paterna, Spain
E-mail: daniel.aranda@uv.es

Prof. M. Kertesz
Department of Chemistry and Institute of Soft Matter, Georgetown University, Washington, D.C.-20057-1227, United States
E-mail: kertesz@georgetown.edu

[+] F.G.G and Y.G contribute equally to this article.

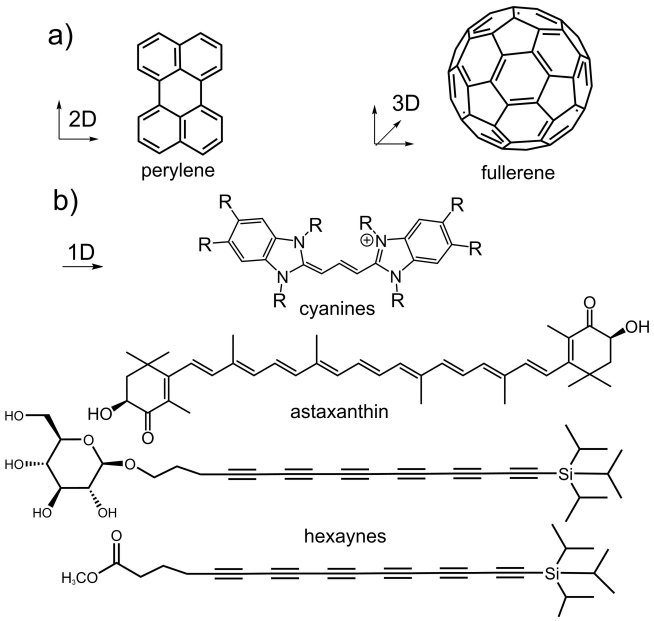

Figure 1. a) Examples of 2D (perylene) and 3D (fullerene) molecules showing aggregation. b) Examples of 1D molecules, such as cyanines and oligoenes, as well short oligoynes, displaying aggregation phenomena.

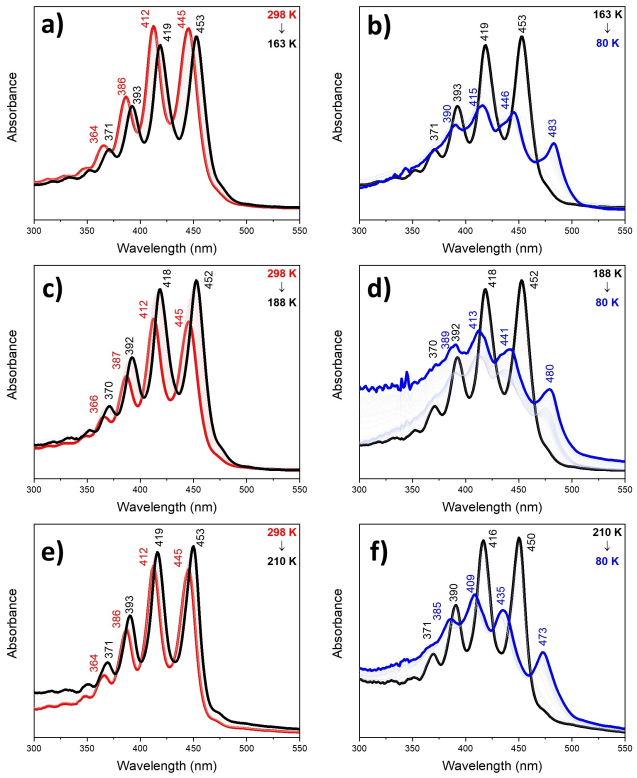

Figure 2. Electronic absorption spectra of **Py[16]** 10^{-5} M at two temperature intervals: 298 K (red lines), 163/188/210 K (black lines), and 80 K (blue lines), as measured in a, b) 2-MeTHF; c, d) 40:60 (2-MeTHF/MCH; mole fraction); and e,f) MCH. Spectra in a), b), e), and f) have been corrected to account for thermal solvent shrinking. A complete description for the temperature dependent measurements can be found in the Supporting Information. Baseline perturbation in the short wavelength region in Figure 2d could be due to co-solvent crystallization, which does not affect the profile of the absorption band in discussion.

Although aggregation of 1D molecules might be unusual, there are representative examples in the literature with different origins (e.g., cyanines[11,12] and oligoenes[13,14] as shown in Figure 1). In the case of cyanines, Coulombic attraction by dipole-dipole interactions is the main driving force for aggregation. The case of oligoenes is more similar to that of oligoynes, and the reported cases (e.g., astaxanthin[15] in Figure 1) demonstrate that terminal endgroups play a key role. Similarly to oligoenes, aggregation of oligoynes (e.g., hexaynes in Figure 1) has been reported,[16] driven by amphiphilic endgroups that are responsible for the self-assembly in polar media.

Herein, we show that solutions of **Py[16]** at low temperature feature the formation of H-type aggregates,[17] which emerge on cooling due to the subtle stabilization by van der Waals interactions between the oligoyne π-wires. This study reveals the unique case of aggregation by π–π 1D enthalpic effects that are able to overcome the entropic cost necessary to produce a favorable scenario for assembly. The experimental results are supported by theoretical modelling calculations of the spectroscopic properties of the individual molecules and the aggregated species using Spano's approach.[13,14,17]

Figure 2 displays the electronic absorption spectra recorded for **Py[16]** at different temperatures in 2-methyltetrahydrofuran (2-MeTHF), 2-MeTHF/MCH 40:60 molar fraction mixtures, and methyl-cyclohexane (MCH). At 298 K, the spectra all show the well-known array of vibronic bands of the main electronic excitation, assignable to the $S_0 \rightarrow S_3$ transition of oligoynes (at 445, 412, 386, and 364 nm in 2-MeTHF).[18] The vibronic progression has a spacing of ~1800 cm^{-1} by which the first two absorptions at 445 and 412 nm are assigned to the 0–0 and 0–1 vibronic components, respectively. Time-dependent density functional theory (TD-DFT) calculations performed at the CAM-B3LYP/6-31G(d,p) level predict the very bright electronic transition (vertical excitation) at 377 nm for **Py[16]** in nice agreement with previous reports on oligoynes[18] (see the Supporting Information for full computational details). This transition is indeed the only bright state amongst the 50 lowest-energy singlet states in the calculation (up to 256 nm) and, therefore, this excitation is responsible of the entire absorption envelop in the experiments in this spectral region. The vibronic shape computed for this main band (377 nm), with peaks at 405, 371, 343 and 318 nm, is comparable with the experimental spectrum recorded for **Py[16]** at 298 K in 2-MeTHF (Figure 3a and Figure S1). Hence, in the follow discussion, this spectrum corresponds to the molecularly dissolved species of **Py[16]**, the monomer.

In all the three solvents, 2-MeTHF, 2-MeTHF/MCH (40:60), and MCH, lowering the temperature produces a red-shift of all the absorption peaks due to the progressive decrease of both thermal energy and contributions from

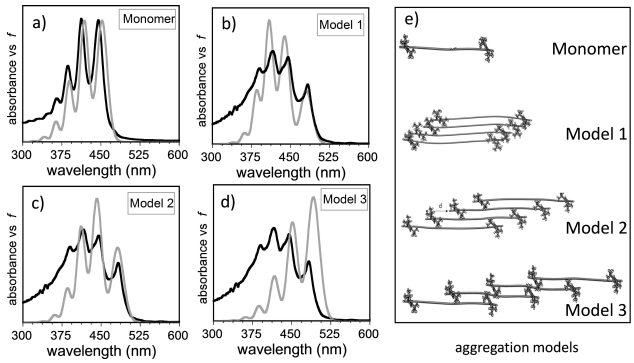

Figure 3. Comparison of the theoretical spectra calculated for different species of **Py[16]** (grey lines) and the experimental UV/Vis spectra recorded in 2-MeTHF for **Py[16]** (black lines). a) monomer at 298 K. b) Aggregate using *Model 1* at 80 K. c) Aggregate using *Model 2* at 80 K. d) Aggregate using *Model 1* at 80 K. e) Representation of the tetramer *Models 1–3* used in the theoretical calculations in comparison to the monomer. The spectra of the aggregates were calculated using a vibronic Hamiltonian whose parameters were fitted to reproduce the experimental spectrum of the monomer as in panel a (see the Supporting Information for full computational details).

solvent-solute interactions. This consistent spectral red-shift is a common feature of organic chromophores on cooling in solution and is progressively observed for **Py[16]** down to approximately 160–210 K depending on the solvent (Figures 2a,c,e). Continued cooling below 160–210 K gives rise to profound changes in the absorption spectra (Figures 2b,d,f, respectively). Measurements in 2-MeTHF are instructive (Figure 2b), since similar changes are observed in MCH and 2-MeTHF/MCH mixtures (Figure 2e and 2d, respectively). The 0–0 vibronic band at 453 nm is the strongest at 163 K, and it concomitantly decreases in intensity upon cooling to 80 K. Concurrently, two new absorptions at 483 and 446 nm emerge through a blue-shifted isosbestic point around 460 nm. The well-resolved isosbestic point is consistent with the equilibrium of different species as the solution is cooled. The process is completely reversible, and warming the solution from 80 to 298 K recovers the starting absorption spectrum. The process of cooling can be followed by representing the variation of the total absorbance at 453 and 483 nm as a function of temperature in 2-MeTHF (Figure S2). The point at which both curves cross corresponds to the transition temperature, which varies as function of the solvent from 146 K in 2-MeTHF, to 160 K in a 40:60 2-MeTHF/MCH, and to 185 K in MCH. This variation suggests the presence of an aggregation process and the role of solvation-desolvation effects. The variable-temperature UV/Vis absorption spectra have also been recorded for the shorter oligoynes in the series **Py[*n*]** ($n=4$, 6, 8, 10, and 12) in the range of 298–80 K (Figure S3). Apart from a red-shift upon decreasing the temperature, as described above for **Py[16]**, no other significant changes are observed for these other oligoynes; i.e., no evidence of self-assembly is observed. The lack of aggregation of shorter oligoynes supports the necessity for a suitable balance of enthalpic and entropic factors that is only achieved at the length of **Py[16]**.

The changes in relative intensities of the vibronic 0–0 and 0–1 components observed for **Py[16]** upon cooling from 163 to 80 K are characteristic of H-type aggregation. The maximum of the spectrum is shifted from the 0–0/0–1 vibronic bands at 453 and 419 nm at 163 K to the 0–1/0–2 band at 446 nm and 415 nm at 80 K, resulting in a blueshift as expected from Kasha's model (Figure 2b). The behaviour is the same in other solvents (Figure 2d,e). Indeed, similar UV/Vis spectral patterns have been reported for oligoenic carotenoids.[13–15] In addition, the occurrence of a spectral red-shift for specific vibronic bands, e.g., the 0–0 band shifting from 453 to 483 nm upon cooling from 163 to 80 K is also consistent not in contradiction with the formation of H-type aggregates because the maximum of the full band is shifted to the blue as discussed above (see the Supporting Information for details). Crystal packing can be used to explore potential aggregation patterns.[13,14] In the series **Py[*n*]**, octayne **Py[8]** is the longest oligoyne for which the crystal structure is resolved (Figure S4),[3] and this structure is therefore taken as a starting point. The solid-state structure of **Py[8]** consists of a stacked arrangement of oligoyne chains, in which each monomer is displaced by ~11 Å along the long wire axis with respect to the next molecule in the stack (Figure S4). The molecular offset places the endgroup of one oligoyne over approximately the center of the sp-carbon core of the neighboring oligoyne along the crystallographic a-axis. Extrapolating from the solid-state structure of **Py[8]**, aggregates were modeled for **Py[16]** by considering an ensemble of four stacked molecules (tetramers) with varied displacement along the oligoyne chain direction (c-axis) as shown in Figure 3e and Figure S5. *Model 1* has a displacement distance of 5.5 Å and displays contacts between the terminal groups of adjacent molecules. *Model 2* separates the bulky endgroups by locating them at approximately one-fourth the distance along the oligoyne chain (11 Å, as observed for **Py[8]**). *Model 3* places the terminal endgroups at the middle of the adjacent **Py[16]** chains (22 Å, the analogous relative offset as observed for **Py[8]**).

To simulate the spectra of the aggregate, the parameters utilized in the excitonic Hamiltonian have been obtained by reproducing the experimental spectrum of the monomer. The agreement between the fit and by the experimental spectra (Figure 3a) validate the selection of parameters (see Table S1). Using these parameters and the excitonic couplings obtained for the decamers (Table S2 and Figure S5), the electronic spectra are computed for the aggregates in *Models 1–3* (see the Supporting Information for full details) and are compared with the experimental spectra at 80 K in Figure 3 and Figure S6. Among the three models, both *Models 1* and *2*, and particularly *Model 1*, fit nicely to the experimental vibronic spectra of the species formed at 80 K. It is noted, furthermore, that the experimental spectra (80 K) all exhibit spectral broadening of the vibronic bands in comparison to the dissolved monomer and calculated spectra, which suggests disorder within the aggregated species. This disorder can likely be attributed to a distribution of the sliding distances between monomers in the

supramolecular aggregate, i.e., a distribution of structures between *Models 1* and *2*.

The overlap between the experimental bands recorded at 446/446 nm and 480/483 nm (at 120/85 K in Figure S7) for the monomeric and aggregated species, respectively, makes the evaluation of their integrated absorbances challenging. Nevertheless a van't Hoff plot of the equilibrium constant as a function of 1/T by assuming a dimerization reaction of **Py[16]** at low temperature can be calculated (Figure S8 and Table S3). In 2-MeTHF, from this analysis, the standard enthalpy, $\Delta H°$, for the dimerization process is estimated to be only $-0.23\ \mathrm{kcal\,mol^{-1}}$. Alternatively, given the plausible formation of multi-molecular aggregates, the energetic parameters of the supramolecular association process at low temperature can be estimated by fitting the logarithmic plot of the absorbances (Figure S2 and Table S4) in the temperature range near the critical transition temperature to a kinetic model of aggregation.[19] This fitting provides an enthalpic estimate of ca. $-4.3\ \mathrm{kcal\,mol^{-1}}$ in 2-MeTHF (Table S5). However, these two estimates of $\Delta H°$ are qualitative and should be viewed as limiting values for the aggregation of **Py[16]** since the significant band overlaps preclude a more accurate analysis. Most importantly, both estimates document an exothermic process. The exothermic nature of aggregation is supported by the theoretical analysis of the energetics of the stacked aggregates, which predicts that the total interaction energy in the formation of a dimer amounts to $-17.7\ \mathrm{kcal\,mol^{-1}}$, from which about $-7.9\ \mathrm{kcal\,mol^{-1}}$ is due to the oligoyne π–π wire contacts (see the Supporting Information for details). This value is expected to be smaller for shorter oligoynes and might be related to the lack of observation of aggregation for oligoynes shorter than **Py[16]**.

Analyses have been carried out using variable-temperature Raman spectra of **Py[16]** in both 2-MeTHF and MCH with Raman excitation lines at 532 and 473 nm (Figure 4 and Figure S9). When using the 473 nm laser excitation, the recorded Raman spectrum is in resonance with the absorption band of the aggregated species absorbing at 483 nm in 2-MeTHF and at 473 nm in MCH. In contrast, laser Raman excitation at 532 nm is out of resonance from the strongest absorptions of both monomeric and aggregated species. By recording the Raman spectrum in resonance with a given absorption, one would expect to obtain the Raman vibrational spectrum of the chromophore to which the excited absorption belongs, based on the strong enhancement (up to factors of 10^6) of the Raman signal when resonance Raman conditions are fulfilled.[20] In addition, the Raman spectra of the **Py[16]** monomer and a dimer with the self-assembled structure of *Model 2* have been calculated (Figure S10). As displayed in Figure 4a, the theoretical spectrum of the monomer shows a main band at $1902\ \mathrm{cm^{-1}}$, due to a symmetric delocalized stretching mode of the triple bonds, ν(C≡C),[3,21,22] whereas the ν(C≡C) band moves to lower wavenumbers at $1887\ \mathrm{cm^{-1}}$ for the aggregated *Model 2* dimer species.

The inherent weakness of the Raman signal forces us to use solution concentrations ($\sim10^{-2}/10^{-3}$ M) that largely exceed those used in the UV/Vis absorption experiments

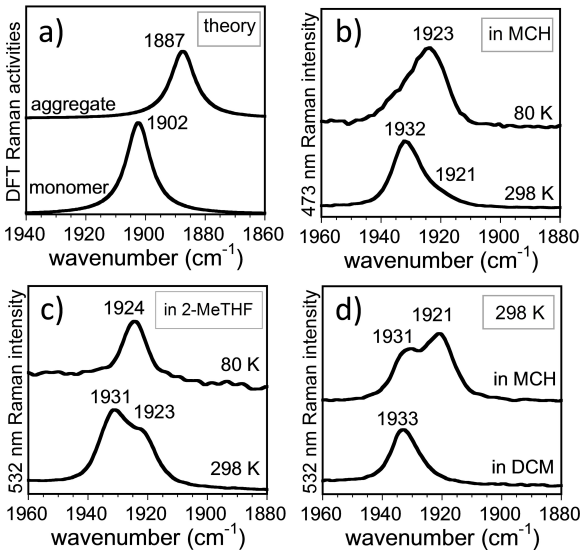

Figure 4. a) Theoretical Raman spectra of the monomer and aggregate species of **Py[16]**. b) Raman spectra of **Py[16]** in MCH ($\sim10^{-3}$ M) at 298 and 80 K (excitation 473 nm). c) Raman spectra of **Py[16]** in 2-MeTHF ($\sim10^{-2}$ M) at 298 and 80 K (excitation 532 nm). d) Raman spectra of **Py[16]** in CH_2Cl_2 (10^{-3} M) and MCH ($\sim10^{-2}$ M) at 298 K (excitation 473 nm).

($\sim10^{-5}$ M). In these conditions, the existence of some fraction of aggregates even at 298 K is possible. Indeed, the Raman spectrum of **Py[16]** at 298 K in MCH with excitation at 473 nm at 10^{-3} M (Figure 4b) has the main band at $1932\ \mathrm{cm^{-1}}$ that correlates with the theoretical band calculated at $1902\ \mathrm{cm^{-1}}$ of the monomer. Yet, there is a small shoulder at $1921\ \mathrm{cm^{-1}}$ that can be related to the aggregate species (i.e., theoretically in the *Model 2* dimer at $1887\ \mathrm{cm^{-1}}$) whose Raman spectrum is enhanced by resonance of the 473 nm laser line with the aggregate absorption band at 483 nm. Further support of this assignment is given the agreement of the overall wavenumber downshift between experiment, $11\ \mathrm{cm^{-1}}$ ($1932\rightarrow1921\ \mathrm{cm^{-1}}$ in MCH) and theory, $15\ \mathrm{cm^{-1}}$ ($1902\rightarrow1887\ \mathrm{cm^{-1}}$). In line with this, at 80 K in MCH with 473 nm excitation, the Raman spectrum shows a main peak at $1923\ \mathrm{cm^{-1}}$ of the aggregate.

Excitation of **Py[16]** at 532 nm in 2-MeTHF at 10^{-2} M at 298 K (Figure 4c) again displays the monomer and aggregate Raman bands at 1931 and $1923\ \mathrm{cm^{-1}}$, respectively, given the high concentration of the solution. Cooling to 80 K results in one band, that of the aggregated species at $1924\ \mathrm{cm^{-1}}$. Finally, the Raman spectrum in CH_2Cl_2 at 10^{-3} M at 298 K in Figure 4d shows the Raman band of the molecularly dissolved species at $1933\ \mathrm{cm^{-1}}$ in agreement with this being a good solvent (i.e., no aggregation).

In conclusion, the unexpected aggregation in solution of a 1D oligoynic chain composed of 16 contiguous triple carbon-carbon bonds is described. With the existing series of oligoynes endcapped with 3,5-bi(3,5-bis-tert-butylphenyl)pyridine groups, the aggregation is unique for **Py[16]** and is not observed for shorter members. The aggregation of **Py[16]** is quite unusual, given the entropic cost for self-assembly of a flexible, conjugated 1D molecule

with very limited π–π surfaces to promote aggregation. The aggregation of **Py[16]** has been monitored by electronic UV/Vis and vibrational Raman spectroscopies as a function of temperature in several solvents. A combined theoretical approximation (quantum-chemical calculations of the monomer and aggregated models as well as excitonic model Hamiltonian calculations including vibronic effects) is employed to offer structural supramolecular models and to understand the experimental spectroscopic results.

The reversible aggregation of **Py[16]** demonstrated in this work could have important implications in the light of the limited details concerning the reactivity of oligoynes. The instability of long oligoynes, and by extension of carbyne, has traditionally been ascribed to their increased tendency to polymerize, particularly for unfunctionalized oligoynes. These reactions are typically promoted by suitable aggregation of intermediate states that facilitate the intermolecular reaction.[23,24] Our observations of reversible aggregation for **Py[16]** opens the door toward understanding the stability and decomposition of oligoynes in a different scenario. Indeed, the ability to form ordered assembly of oligoynes should contribute to the discovery of unknown properties of oligoynes.

Acknowledgements

Financial support by the MCIN/AEI of Spain (projects PID2021-127127NB-I00, PID2021-128569NB-I00, and CEX2019-000919-M, funded by MCIN/AEI/10.13039/501100011033 and by "ERDF A way of making Europe"), the Generalitat Valenciana (MFA/2022/017) and the Junta de Andalucía (PROYEXCEL-0328) is acknowledged. The MFA/2022/017 project forms part of the Advanced Materials programme supported by MCIN with funding from European Union NextGenerationEU (PRTR-C17.I1) and by Generalitat Valenciana. This material is partly based on work supported by the U.S. Department of Energy, Office of Science, Office of Basic Energy Sciences under Award Number DE-SC-0019017 to M.K. Financial support of this work from the Natural Sciences and Engineering Research Council of Canada (R.R.T.), and the Canada Foundation for Innovation (R.R.T.) is gratefully acknowledged. J.A. is indebted to the MCIN/AEI for his Ramón-y-Cajal (RyC-2017-23500) fellowship funded by MCIN/AEI/10.13039/501100011033 and by "ESF Investing in your future". D.A. acknowledges the Generalitat Valenciana and the Spanish Government/NextGenerationUE fundings for his postdoctoral contract (APOSTD/2021/025). We also thank the Research Central Services (SCAI) and Supercomputing and Bioinnovation Center (SCBI) of the University of Málaga.

Conflict of Interest

The authors declare no conflict of interest.

Data Availability Statement

The data that support the findings of this study are available in the supplementary material of this article.

Keywords: one-dimensional wires · oligoynes · aggregation · H-type aggregates

[1] Y. Gao, R. R. Tykwinski, *Acc. Chem. Res.* **2022**, *55*, 3616–3630.
[2] E. M. Shustorovich, N. M. Popov, *Zh. Strukt. Khim.* **1965**, *6*, 596–604; S. Yang, M. Kertesz, V. Zólyomi, J. Kürti, *J. Phys. Chem. A* **2007**, *111*, 2434–2441; F. Banhart, *ChemTexts* **2020**, *6*, 1–10.
[3] Y. Gao, Y. Hou, F. Gordillo Gámez, M. J. Ferguson, J. Casado, R. R. Tykwinski, *Nat. Chem.* **2020**, *12*, 1143–1149.
[4] A. Arora, S. D. Baksi, N. Weisbach, H. Amini, N. Bhuvanesh, J. A. Gladysz, *ACS Cent. Sci.* **2023**, *9*, 2225–2240; C. W. Patrick, Y. Gao, P. Gupta, A. L. Thompson, A. W. Parker, H. L. Anderson, *Nat. Chem.* **2024**, *16*, 193–200.
[5] L. Zang, Y. Che, J. S. Moore, *Acc. Chem. Res.* **2008**, *41*, 1596–1608.
[6] Y. Gu, Z. Qiu, K. Müllen, *J. Am. Chem. Soc.* **2022**, *144*, 11499–11524; J. Wu, W. Pisula, K. Müllen, *Chem. Rev.* **2007**, *107*, 718–747.
[7] R. F. Fink, J. Seibt, V. Engel, M. Renz, M. Kaupp, S. Lochbrunner, H. M. Zhao, J. Pfister, F. Würthner, B. Engels, *J. Am. Chem. Soc.* **2008**, *130*, 12858–12859.
[8] D. Wasserfallen, M. Kastler, W. Pisula, W. A. Hofer, Y. Fogel, Z. Wang, K. Müllen, *J. Am. Chem. Soc.* **2006**, *128*, 1334–1339.
[9] N. O. Mchedlov-Petrossyan, *Chem. Rev.* **2013**, *113*, 5149–5193.
[10] S. Szafert, J. A. Gladysz, *Chem. Rev.* **2006**, *106*, PR1–PR33.
[11] F. Würthner, T. E. Kaiser, C. R. Saha-Möller, *Angew. Chem. Int. Ed.* **2011**, *50*, 3376–3410.
[12] Z. Li, S. Mukhopadhyay, S. H. Jang, J. L. Brédas, A. K. Y. Jen, *J. Am. Chem. Soc.* **2015**, *137*, 11920–11923.
[13] F. C. Spano, *J. Am. Chem. Soc.* **2009**, *131*, 4267–4278.
[14] F. C. Spano, *Acc. Chem. Res.* **2010**, *43*, 429–439.
[15] A. J. Musser, M. Maiuri, D. Brida, G. Cerullo, R. H. Friend, J. Clark, *J. Am. Chem. Soc.* **2015**, *137*, 5130–5139.
[16] S. Schrettl, E. Contal, T. N. Hoheisel, M. Fritzsche, S. Balog, R. Szilluweit, H. Frauenrath, *Chem. Sci.* **2015**, *6*, 564–574.
[17] N. J. Hestand, F. C. Spano, *Chem. Rev.* **2018**, *118*, 7069–7163.
[18] J. Zirzlmeier, S. Schrettl, J. C. Brauer, E. Contal, L. Vannay, É. Brémond, E. Jahnke, D. M. Guldi, C. Corminboeuf, R. R. Tykwinski, H. Frauenrath, *Nat. Commun.* **2020**, *11*, 1–10.
[19] H. M. M. Ten Eikelder, A. J. Markvoort, T. F. A. De Greef, P. A. J. Hilbers, *J. Phys. Chem. B* **2012**, *116*, 5291–5301.
[20] D. A. Long, *The Raman Effect*, John Wiley and Sons, **2002**, Chichester, UK.
[21] A. Milani, M. Tommasini, V. Barbieri, A. Lucotti, V. Russo, F. Cataldo, C. S. Casari, *J. Phys. Chem. C* **2017**, *121*, 10562–10570.
[22] A. Lucotti, M. Tommasini, D. Fazzi, M. Del Zoppo, W. A. Chalifoux, M. J. Ferguson, G. Zerbi, R. R. Tykwinski, *J. Am. Chem. Soc.* **2009**, *131*, 4239–4244.
[23] M. R. Bryce, *J. Mater. Chem. C* **2021**, *9*, 10524–10546.
[24] E. Bomal, P. Grandgeorge, R. J. Yeo, N. Candau, P. M. Reis, H. Frauenrath, *Nat. Commun.* **2022**, *13*, 4950.

Manuscript received: February 27, 2024
Accepted manuscript online: June 27, 2024
Version of record online: August 19, 2024